American Mineralogist, Volume 91, pages 1211–1215, 2006

Low-temperature Zr mobility: An in situ synchrotron-radiation XRF study of the effect of radiation damage in zircon on the element release in H_2O + HCl ± SiO_2 fluids

CHRISTIAN SCHMIDT,[1,*] KAREN RICKERS,[1,2] RICHARD WIRTH,[1] LUTZ NASDALA,[3,†] AND JOHN M. HANCHAR[4]

[1]GeoForschungsZentrum Potsdam, Telegrafenberg, D-14473 Potsdam, Germany
[2]Hamburger Synchrotronstrahlungslabor at Deutsches Elektronen-Synchrotron DESY, Notkestr. 85, D-22607 Hamburg, Germany
[3]Institut für Geowissenschaften—Mineralogie, Johannes Gutenberg-Universität, Becherweg 21, D-55099 Mainz, Germany
[4]Department of Earth Sciences, Memorial University of Newfoundland, St. John's, Newfoundland, A1B 3X5, Canada

ABSTRACT

The release of Zr, U, and Pb from nearly metamict zircon and its recrystallized analog and of Zr from fully crystalline and slightly radiation-damaged zircon in H_2O + HCl ± SiO_2 fluids was investigated in situ at temperatures between 200 and 500 °C using a hydrothermal diamond-anvil cell and time-resolved synchrotron-radiation XRF analyses. Dissolution of nearly metamict zircon proceeded much faster than that of zircon with little or no radiation damage and resulted in a 1.5 to 2 log units higher Zr molality in 6 to 7 *m* HCl fluids. Extensive recrystallization of the almost fully amorphous material started at 260 to 300 °C in H_2O + HCl, and at about 360 °C if quartz was added, and was coupled with a decrease of the Zr concentration in the fluid by more than an order of magnitude. Recrystallization in 7 *m* HCl had little effect on the aqueous U and Pb concentrations, whereas addition of quartz caused a more sluggish decrease of the Zr concentration in the fluid upon recrystallization and lowered the release of U. The data presented here support the interpretation that enhanced Zr mobility in low-grade metamorphic rocks may be related to dissolution of metamict zircon by aqueous fluids and illustrate the significance of the silica activity on the kinetics of dissolution and recrystallization during zircon-fluid interaction.

Keywords: High-temperature studies, zircon-aqueous fluid interactions, hydrothermal diamond-anvil cell, in-situ SR-XRF analysis, dissolution kinetics, order-disorder, metamictization, recrystallization, fluid phase, H_2O + HCl ± SiO_2, recrystallization kinetics

INTRODUCTION

The accessory mineral zircon, $ZrSiO_4$, is the main host of Zr in the Earth's crust. It incorporates Hf, U, Th, and other trace elements, but is highly incompatible for Pb^{2+} during crystallization. Thus, zircon is an important source of geochronological and geochemical information to unravel the evolution of the lithosphere. The Earth's oldest known rocks have been dated based on zircon geochronology, which also points toward the remarkable chemical and physical stability of this mineral (e.g., Ireland and Williams 2003). Although zirconium can be considered as an immobile element under many crustal conditions, there is growing evidence that enhanced mobility induced by aqueous fluids is more abundant than previously thought. Metamorphic zircon overgrowths on detrital zircon grains and, less common, partial dissolution of zircon grains have been observed in many Archean to Paleozoic low-grade metasedimentary rocks worldwide, in greenschist-facies slates at temperatures ≤350 °C (Dempster et al. 2004) and in prehnite-pumpellyite facies shales, in which zircon growth commenced at about 250 °C (Rasmussen 2005). This unexpected low-temperature mobility of Zr has been related to the dissolution and recrystallization of metamict portions in zircon grains (Dempster et al. 2004). Metamictization, i.e., the transformation from the crystalline to a metastable amorphous state, is due to the radioactive decay of U and Th and their unstable daughter isotopes (e.g., Ewing et al. 2003). Structural damage is caused mainly by recoils of heavy daughter nuclei upon emission of an α-particle. Damage accumulation results in a higher susceptibility of zircon to alteration by aqueous fluids, which has been long known from hydrothermal experiments (Pidgeon et al. 1974). Most studies on the hydrothermal alteration of zircon focused on the solid phases, particularly because of the important consequences in geochronology (e.g., Pidgeon et al. 1974; Levchenkov et al. 1998; Geisler et al. 2003). The available experimental information on solubility and dissolution kinetics of zircon in aqueous fluids is still limited (e.g., Ayers and Watson 1991; Newton et al. 2005). These studies demonstrate that the silica release upon zircon dissolution in water is controlled via the reaction $ZrSiO_4(s) = ZrO_2(s) + SiO_2(aq)$. The difference in the element release from amorphous and crystalline zircon in aqueous fluids has rarely been quantified, e.g., Ewing et al. (1982) measured the Zr concentration in 5 wt% $KHCO_3$ solutions after reaction with zircon at 87 °C for 9.9 days and calculated bulk leach rates for metamict samples, which were by 1 to 2 orders of magnitude higher than those of crystalline zircon.

In this paper, we present experimental results on Zr and,

* E-mail: hokie@gfz-potsdam.de
† Present address: Institut für Mineralogie und Kristallographie, Universität Wien, Althanstr. 14, A-1090 Wien, Austria

0003-004X/06/0809–1211$05.00/DOI: 10.2138/am.2006.2244

where detectable, the U and Pb concentrations in H_2O + HCl fluids during interaction with crystalline or metamict (nearly amorphous) natural and synthetic zircon. The concentrations of those elements in the fluid were obtained as a function of time at temperatures between 200 and 500 °C using a hydrothermal diamond-anvil cell and time-resolved synchrotron-radiation X-ray fluorescence (SR-XRF) analyses. This technique has a distinct advantage for studying the kinetics of zircon-fluid interaction because it permits in situ monitoring of the aqueous concentrations of heavy elements released from a mineral at high temperatures and pressures, i.e., quenching is not required for analysis of the fluid (Schmidt and Rickers 2003). Because zircon dissolves incongruently and upper crustal fluids are likely saturated in SiO_2, the silica activity in the fluid was buffered in some experiments by addition of quartz to observe the effect on element release and recrystallization kinetics.

Experimental procedure

Three well-characterized zircon samples without notable heterogeneity were used: a synthetic pure $ZrSiO_4$ single crystal (Hanchar et al. 2001) and two gem-quality zircon samples from Sri Lanka. The latter included the nearly amorphous sample N17, containing 5568 ± 89 ppm U, 344 ± 30 ppm Th, and 453 ± 23 ppm Pb (Nasdala et al. 2002) and sample M144, which displayed little radiation damage and had average contents of 436 ± 7 ppm U, 140 ± 3 ppm Th, and 39 ± 1 ppm Pb (Nasdala et al. 2004).

The hydrothermal experiments were done at the SR-XRF microprobe at the Hamburger Synchrotronstrahlungslabor at beamline L of DORIS III at DESY, Hamburg, Germany. All XRF spectra were collected using an HPGe energy-dispersive detector aligned at 90° to the beam in the polarization plane of the incident X-rays. A pink multilayer beam with photon energies of 22.3 ± 0.1 keV was used for excitation, and a single bounce capillary to increase the flux density and to focus the beam into a spot of 11 ± 1 µm at a focal distance of 5 cm (Huang and Bilderback 2006). This setup is optimized for the detection of elements with emission lines in the energy range from 12 to 20 keV in HDAC-confined samples. In our experiments, the lower limits of detection were 1–2 ppm for Zr, 1–3 ppm for U, and 2–5 ppm for Pb.

Externally heated Bassett-type hydrothermal diamond-anvil cells (HDAC) (Bassett et al. 1993) were employed for the experiments. The design of these cells was modified to facilitate in situ SR-XRF analyses of fluids at temperatures to 800 °C and pressures to about 2 GPa (Schmidt and Rickers 2003). A zircon chip (maximum diameter ≈100 µm) and a H_2O + 3 *m* HCl solution (*m* denotes moles of solute per kg of H_2O) were loaded into the sample chamber of the cell, which consisted of a 400 or 500 µm hole in an Ir gasket separating two diamond anvils. In some experiments, a quartz crystal (size ≈ 100 µm) was added. Before the sample chamber was sealed by compression of the gasket between the anvils, some liquid was allowed to slowly leak out until the size of the produced air bubble was sufficient to attain a fluid bulk density of about 0.9 g/cm^3. Because a significant amount of water evaporates during loading of the fluid and controlled leaking, the actual HCl concentration in the sealed sample chamber was determined via measurement of the ice melting temperature in the presence of vapor.

The cell was then mounted on the xyz-stage of the SR-XRF spectrometer and heated to the first experimental temperature. The portion of the fluid to be analyzed (i.e., of the liquid phase if vapor was present, or of the single-phase fluid at temperatures above liquid-vapor homogenization) was aligned to the beam and the fluorescence detector. After alignment, consecutive SR-XRF spectra were recorded in situ to determine the concentrations of Zr, U, and Pb in the solution as a function of time. Subsequently, the liquid-vapor homogenization temperature of the fluid was measured in case of experiments above vapor pressure. The sample was then heated to a higher experimental temperature and the cycle described above was repeated. The fluid density and the pressure at the individual run temperatures were calculated from the HCl concentration of the solution and the liquid-vapor homogenization temperature using approximations based on a compilation of available literature data (Schmidt et al., in review).

The Zr, U, and Pb XRF signals that were acquired were calibrated for each experimental series from measurements of aqueous standard solutions containing 10 wt% NaCl and 250 or 1000 µg/g Rb loaded into the HDAC sample chamber. The actual Rb concentration after loading was determined from the ice melting or the halite dissolution temperature in the presence of vapor. All recorded spectra were normalized to 100 mA DORIS III current and a live time of 1000 seconds and processed using the software package AXIL (Vekemans et al. 1995, 2004). The Zr, U, and Pb peak areas that were obtained were divided by the fluid density at the experimental *P-T* conditions and converted to molal concentrations based on the density-normalized Rb Kα peak areas from the spectra of the standard solutions, and on Zr/Rb, U/Rb, and Pb/Rb correction factors. These correction factors relative to the reference element Rb were obtained for each HDAC from measurements of a standard solution containing 250 mg U, 250 mg Pb, 250 mg Zr, and 250 mg Rb per liter solution loaded into the sample chambers.

The degree of zircon metamictization before and after hydrothermal treatment was estimated from the full width at half maximum (FWHM) of the $\nu_3(SiO_4)$ Raman band at about 1000 cm^{-1} (Nasdala et al. 1995, 2002). The Raman spectra were recorded using a Dilor XY Raman microprobe (gratings 1800 lines/mm, focal length 800 mm) equipped with a CCD-detector. The slit width was 100 µm and the spectral resolution s = 0.62 cm^{-1}. The power of the 488 nm excitation line of the Ar^+ laser was less than 12 mW at the sample to avoid band broadening due to sample heating from the laser. Two microscope objectives were used: an Olympus 80× (numerical aperture 0.75) or, if the zircon was still in the sealed sample chamber of the HDAC, a Nikon 20× SLWD (numerical aperture 0.35).

Using the focused ion beam technique (Wirth 2004), thin foils were cut from sample N17 before and after recrystallization in 7.0 *m* HCl and analyzed by transmission electron microscopy (TEM) to determine the phase assemblage, the crystallinity, and the grain size of the solids after recrystallization.

Results and discussion

The untreated zircon N17 is almost completely amorphous, based on the Raman spectrum (Fig. 1a) and the electron diffraction pattern (Fig. 1b). After recrystallization of this sample in 7.0 *m* HCl, it contained mostly fine-grained zircon crystals having a grain size of approximately 20 to 50 nm (Fig. 1c). Remnants of the amorphous phase were still present after hydrothermal treatment at 450 °C as shown by the energy-filtered lattice fringe image and the high diffuse scattering intensity in the electron diffraction pattern (Fig. 1d). There was no evidence for crystalline ZrO_2 from Raman spectroscopy or TEM. Upon heating sample N17 in H_2O + HCl, the onset of massive recrystallization was recognizable optically by rapid darkening, which was observed at 260 to 300 °C in quartz-absent experiments (Figs. 1e–1g). This darkening is caused by light refraction on the faces of the many nanocrystals formed during recrystallization. Slight structural changes may already have occurred at temperatures <200 °C according to Geisler et al. (2003).

The $\nu_3(SiO_4)$ FWHM in the Raman spectra of sample N17 after the hydrothermal experiments in 7.0 *m* HCl (Fig. 1a) and 4.6 *m* HCl was, in both cases, close to that of fully crystalline zircon, i.e., the fine-grained zircon crystals in the run products displayed little distortion of the SiO_4 tetrahedra (Nasdala et al. 1995). In contrast, the $\nu_3(SiO_4)$ had a significantly larger FWHM after treatment of sample N17 in 6.1 *m* HCl in the presence of quartz. This indicates that the conversion of amorphous to crystalline zircon was less advanced if the fluid was saturated in silica, although the run duration at 450 °C was considerably longer and the HCl concentration was similar to that of the quartz-free experiment. Additionally, the Raman spectra showed an apparent additional band, observed as a shoulder at 425 to 430 cm^{-1}, which was not detectable after quartz-absent experiments (Fig. 1a). The frequency of this signal matches that of the most prominent Raman band of amorphous silica (McMillan 1984).

The Zr und U molalities in the fluid initially increased with time during dissolution of amorphous zircon N17 in 7.0 *m* HCl at 260 °C (quartz-free experiment), until constant concentrations were attained after less than 5000 seconds (Fig. 2a). With the possible exception of one spectrum, the Pb concentration in the fluid was below the lower limit of detection. Recrystallization of the solid at 300 °C was coupled with a large decrease of the Zr concentration in the fluid by more than an order of magnitude

until it became constant after 10 000 seconds. A slightly higher Zr concentration was obtained after subsequent heating to 450 °C (Fig. 2a). However, the uranium molality in the fluid increased continuously, unaffected by recrystallization, from 0.00061 to 0.00074 *m* at 300 °C to 0.00077 *m* at 450 °C, and Pb became detectable in most XRF spectra (Fig. 2a). Therefore, U and Pb released from amorphous zircon in the fluid were not reincorporated in solid phases during the recrystallization process within the duration of our experiments (a few hours). Although the grain size was too small to analyze individual solid phases for U and Pb after the experiment, the bulk solid must have been depleted in both elements because the U/Zr and the Pb/Zr ratios in the fluid are much higher than those in untreated zircon N17 (Fig. 2b). This depletion of the bulk solid in U and Pb relative to Zr was primarily related to recrystallization, whereas the preceding dissolution of the metamict zircon had a smaller effect on the U/Zr and, perhaps, the Pb/Zr ratio (Fig. 2b). In contrast, the Th concentration in the fluid was always below the lower limit of detection ($\approx 1 \cdot 10^{-5}$ *m*), which indicates an increase in the Th/Zr ratio in the solid during dissolution at 260 °C relative to the ratio in the untreated sample. The significantly higher U/Pb ratio in the fluid at 260 °C compared to that of untreated zircon N17 (Fig. 2b) implies a decrease in the U/Pb ratio of the bulk solid during reaction with 7.0 *m* HCl. This can be attributed to

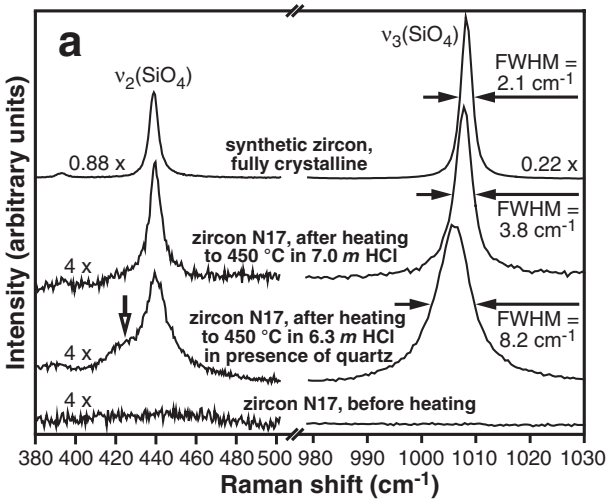

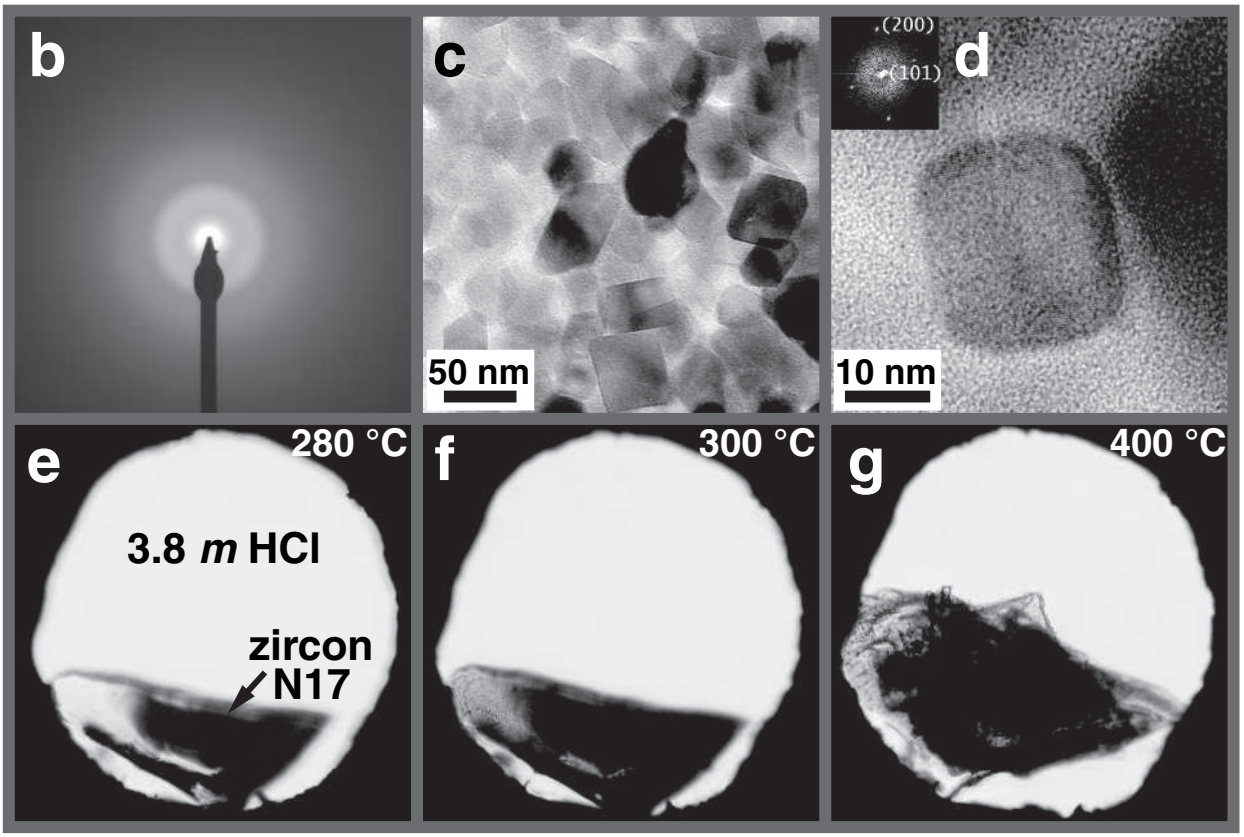

FIGURE 1. (**a**) Raman spectra of zircon N17 at 22 °C and 0.1 MPa before and after recrystallization in H_2O + HCl. Assignment of Raman bands: $\nu_2(SiO_4)$ = symmetric SiO_4 bending, $\nu_3(SiO_4)$ = antisymmetric SiO_4 stretching, shoulder at ≈ 425 cm^{-1} (thick arrow) = amorphous silica. A spectrum of fully crystalline synthetic zircon is given for reference. FWHM = full width at half band-maximum. (**b–d**) TEM images of zircon N17: (**b**) amorphous starting material, electron diffraction pattern; (**c**) and (**d**) after recrystallization in 7.0 *m* HCl at 450 °C, (**c**) bright field image, (**d**) energy-filtered lattice fringe image of zircon nanocrystals in amorphous matrix. Inset: electron diffraction pattern (Fourier transform) of the image. The diffraction pattern corresponds to the two sets of lattice fringes (200) and (101) of the two crystals. The intense diffuse scattering is due to the amorphous matrix. (**e–g**) Plan view of the sample chamber (diameter ≈300 μm) of the hydrothermal diamond-anvil cell during heating of zircon N17 in 3.8 *m* HCl at 280 °C (**e**), 300 °C (**f**), and after 24 minutes at 400 °C (**g**).

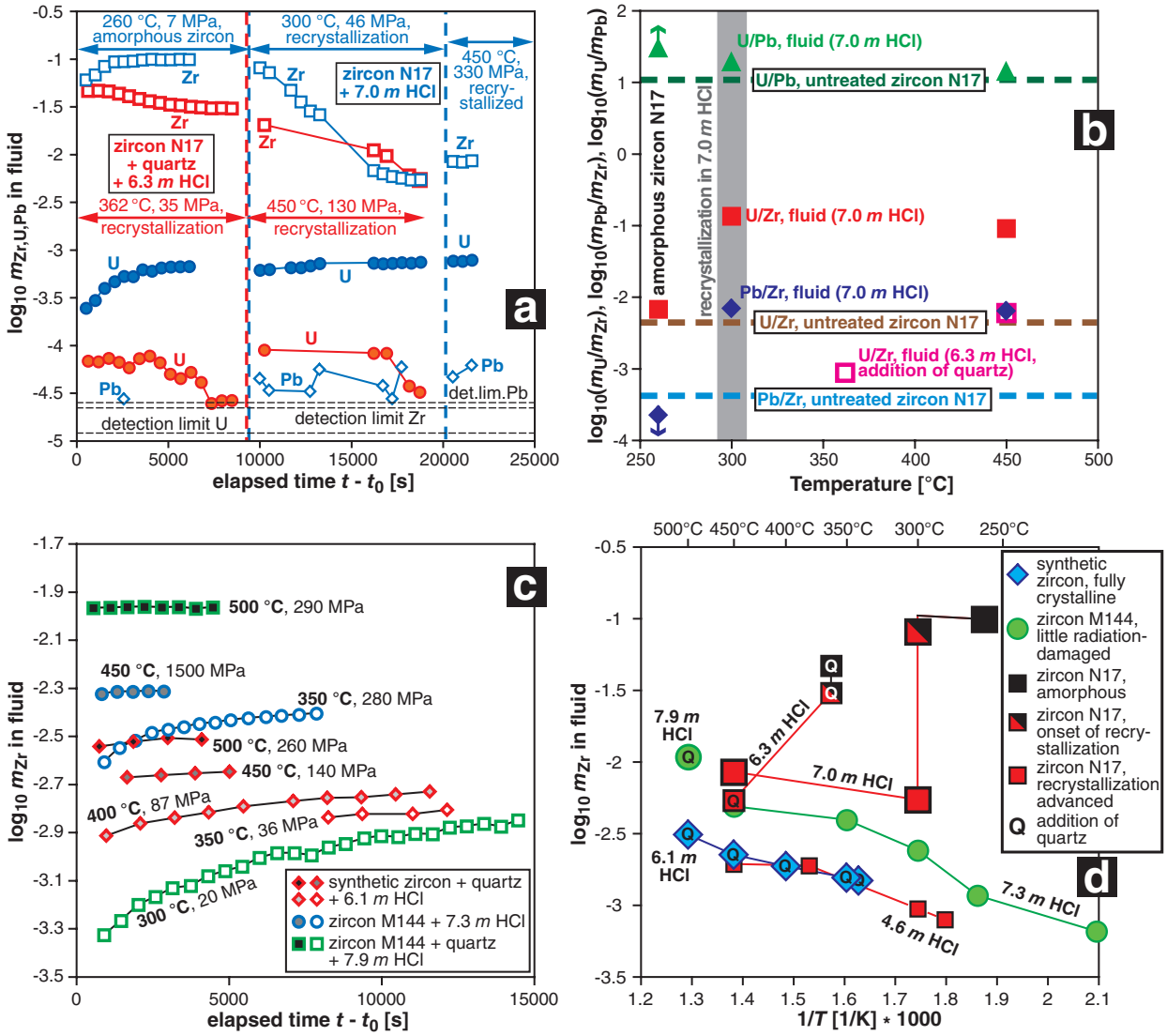

FIGURE 2. Results of the in situ SR-XRF analyses of the fluid during hydrothermal alteration of zircon in H_2O + HCl ± SiO_2. The random error in the concentrations is <1% at m_{Zr} or $m_U > 5 \cdot 10^{-4}$, i.e., smaller than the symbol size, ≈10% at $m_U \approx 1 \cdot 10^{-4}$, ≈25% at $m_U \approx 3 \cdot 10^{-5}$, and ≈50% at $m_{Pb} \approx 4 \cdot 10^{-5}$. (**a**) Temporal evolution of the Zr (squares), U (circles), and Pb (diamonds) concentrations in the fluid during interaction with initially nearly amorphous zircon N17. Red symbols = quartz present; blue symbols = quartz absent; t_0 = time at which heating to the first experimental temperature was completed. (**b**) Comparison of the U/Zr, Pb/Zr, and U/Pb ratios in untreated zircon N17 (dashed lines, data from Nasdala et al. 2002) to the ratios in the fluid during dissolution of zircon N17 (calculated from the last recorded concentrations). U/Pb and Pb/Zr ratios at 260 °C = minimum or maximum estimates based on the lower limit of detection for Pb. (**c**) Temporal evolution of the Zr molality in the fluid during dissolution of zircon with little (M144) or no radiation damage. (**d**) Zirconium concentration in the fluid released from zircon as a function of temperature for different zircon crystallinities, HCl molalities, and silica activities. If equilibrium was not attained during dissolution of synthetic zircon or sample M144, the last Zr concentration recorded at the experimental temperature was plotted as the minimum estimate (cp. **c**).

the high U release in the solution at these conditions, because the behavior of U during hydrothermal alteration of zircon is much more dependent on fluid composition than that of Pb, as demonstrated by several experimental studies (e.g., Pidgeon et al. 1974; Levchenkov et al. 1998).

If quartz was added to the system, the decrease in the Zr concentration in the fluid caused by recrystallization of zircon N17 started at a higher temperature than during the quartz-free experiment in 7.0 *m* HCl, and continued after heating to 450 °C (Fig. 2a). Additionally, the U molality in the fluid was much lower and started to decrease about 2 h after the experimental temperature was attained (Fig. 2a). This was probably due to incorporation as a coffinite ($USiO_4$) component in the zircon or due to precipitation as a separate U-bearing phase. At the end of the run at 450 °C, the U/Zr ratio in the fluid was close to that in untreated zircon N17 (Fig. 2b). Lead was not detectable in the solution. A plausible interpretation of the more sluggish behavior in these experiments is the formation of a silica layer on the surface of amorphous zircon, from which Zr^{4+} is removed during dissolution, but no SiO_2, because the fluid is already saturated

in silica. The onset of the extensive recrystallization created a sharp contrast between the chemical potentials of Zr in the fluid and of Zr in the zircon crystals nucleated in the metamict phase. This acted as the driving force for the diffusion of Zr in the fluid (probably mostly as $Zr(OH)^{2+}$ complexes) toward the zircon. The silica layer on the surfaces, however, likely slowed the backward diffusion of dissolved Zr. This interpretation is supported by the larger amount of amorphous silica in the sample after recrystallization in comparison to the quartz-free run (Fig. 1a).

In comparison to amorphous zircon (Fig. 2a), the dissolution kinetics of fully crystalline and slightly radiation-damaged zircon (Fig. 2c) were considerably more sluggish. At temperatures <450 °C, the aqueous Zr concentration did not become constant within the time available for the experiments. The slightly radiation-damaged sample M144 and the synthetic crystal displayed a similar Zr release behavior as a function of time, temperature, and silica activity in the fluid (Figs. 2c and 2d). The amorphous fraction in zircon M144 is only about 0.14% based on the $\nu_3(SiO_4)$ FWHM, and the amorphous domains are not interconnected (Nasdala et al. 2004). Thus, the contribution of the amorphous phase to the Zr release from M144 was probably too small to cause a noticeable effect.

The difference in the aqueous Zr concentration released from crystalline and amorphous zircon (Δm_{Zr}) was large, about 2 orders of magnitude at 260 °C and ≈ 7 *m* HCl (Fig. 2d). Because equilibrium was not attained during dissolution of synthetic zircon and sample M144 within the available time for the experiments at this temperature, Δm_{Zr} is likely smaller at long run durations. In the case of silica saturation, we observed a similarly large effect (Δm_{Zr} was about 1.5 log units at 360 °C and about 6 *m* HCl). Recrystallized zircon N17 still released more Zr in the fluid than crystalline zircon at similar conditions, although Δm_{Zr} was much smaller (Fig. 2d). This may be related to the fine grain size of the zircon crystals and a remaining small fraction of amorphous phase in the recrystallized samples.

The results of our study support the hypothesis that enhanced Zr mobility in low-grade metamorphic rocks can be attributed to dissolution of metamict zircon by aqueous fluids. Although we used higher HCl molalities than occur in nature, mainly to unambiguously observe the effects on the aqueous Zr and U concentrations in in-situ experiments and to accelerate dissolution kinetics (Schmidt et al., in review), this conclusion can be drawn because the short-range ordering process in recrystallizing zircon was independent of the HCl concentration (Geisler et al. 2003). Furthermore, the temperatures at which massive recrystallization caused a pronounced decrease of the Zr concentration in the aqueous solution are consistent with the temperature range of 250 to 350 °C, which appears to limit increased Zr mobility in metamorphic rocks (Dempster et al. 2004; Rasmussen 2005). The Zr concentration will be much lower in natural fluids compared to that in our experiments, but metamict zircon will, likewise, release Zr far more efficiently than zircon with little radiation damage, and a shorter fluid-zircon interaction time will increase this effect further due to the slower dissolution of crystalline zircon. However, the high Zr concentrations in fluids from dissolution of strongly radiation-damaged zircon are supersaturated with respect to crystalline zircon. It is thus likely that Zr migration over distances well above grain scale is limited because of precipitation on the next crystalline zircon surface.

Acknowledgments

The authors thank Bill Bassett, Peter Dulski, Gerald Falkenberg, Thorsten Geisler, Wilhelm Heinrich, Andrew Putnis, Rolf Romer, Anne-Magali Seydoux-Guillaume, and Rainer Thomas for discussions, support, and assistance with various aspects of this study, HASYLAB at DESY for granting beamtime for this project, and two anonymous reviewers for helpful comments.

References cited

Ayers, J.C. and Watson, E.B. (1991) Solubility of apatite, monazite, zircon, and rutile in supercritical aqueous fluids with implications for subduction zone geochemistry. Philosophical Transactions of the Royal Society of London, A 335, 365–375.

Bassett, W.A., Shen, A.H., Bucknum, M., and Chou, I.-M. (1993) A new diamond anvil cell for hydrothermal studies to 2.5 GPa and from –190 to 1200 °C. Reviews of Scientific Instruments, 64, 2340–2345

Dempster, T.J., Hay, D.C., and Bluck, B.J. (2004) Zircon growth in slate. Geology, 32, 221–224.

Ewing, R.C., Haaker, R.F., and Lutze, W. (1982) Leachability of zircon as a function of alpha dose. In W. Lutze, Ed., Scientific Basis for Radioactive Waste Management V, p. 389–397. Elsevier, Amsterdam.

Ewing, R.C., Meldrum, A., Wang, L.M., Weber, W.J., and Corrales, L.R. (2003) Radiation effects in zircon. In J.M. Hanchar and P.W.O. Hoskin, Eds., Zircon, 53, p. 387–425. Reviews in Mineralogy and Geochemistry, Mineralogical Society of America, Chantilly, Virginia.

Geisler, T., Zhang, M., and Salje, E.K.H. (2003) Recrystallization of almost fully amorphous zircon under hydrothermal conditions: An infrared spectroscopic study. Journal of Nuclear Materials, 320, 280–291.

Hanchar, J.M., Finch, R.J., Hoskin, P.W.O., Watson, E.B., Cherniak, D.J., and Mariano, A.N. (2001) Rare earth elements in synthetic zircon: Part 1. Synthesis, and rare earth element and phosphorus doping. American Mineralogist, 86, 667–680.

Huang, R. and Bilderback, D.H. (2006) Single-bounce monocapillaries for focusing synchrotron radiation: modeling, measurements, and theoretical limits. Journal of Synchrotron Radiation, 13, 74–84.

Ireland, T.R. and Williams, I.S. (2003) Considerations in zircon geochronology by SIMS. In J.M. Hanchar and P.W.O. Hoskin, Eds., Zircon, 53, p. 215–241. Reviews in Mineralogy and Geochemistry, Mineralogical Society of America, Chantilly, Virginia.

Levchenkov, O.A., Rizvanova, N.G., Maslenikov, A.V., Makeev, A.F., Bezmen, N.I., and Levsky, L.K. (1998) Kinetics of Pb and U loss from metamict zircon under different *P-T-X* conditions. Geochemistry International, 36, 1006–1013.

McMillan, P. (1984) Structural studies of silicate glasses and melts—applications and limitations of Raman spectroscopy. American Mineralogist, 69, 622–644.

Nasdala, L., Irmer, G., and Wolf, D. (1995) The degree of metamictization in zircon: a Raman spectroscopic study. European Journal of Mineralogy, 7, 471–478.

Nasdala, L., Lengauer, C.L., Hanchar, J.M., Kronz, A., Wirth, R., Blanc, P., Kennedy, A.K., and Seydoux-Guillaume, A.-M. (2002) Annealing radiation damage and the recovery of cathodoluminescence. Chemical Geology, 191, 119–138.

Nasdala, L., Reiners, P.W., Garver, J.I., Kennedy, A.K., Stern, R.A., Balan, E., and Wirth, R. (2004) Incomplete retention of radiation damage in zircon from Sri Lanka. American Mineralogist, 89, 219–231.

Newton, R.C, Manning, C.E., Hanchar, J.M., and Finch, R.J. (2005) Gibbs free energy of formation of zircon from measurement of solubility in H_2O. Journal of the American Ceramic Society, 88, 1854–1858.

Pidgeon, R.T., O'Neil, J.R., and Silver, R.T. (1974) Observations on the crystallinity and the U-Pb system of a metamict Ceylon zircon under experimental hydrothermal conditions. Fortschritte der Mineralogie, 50, 118.

Rasmussen, B. (2005) Zircon growth in very low-grade metasedimentary rocks: evidence for zirconium mobility at ≈250 °C. Contributions to Mineralogy and Petrology, 150, 146–155.

Schmidt, C. and Rickers, K. (2003) In-situ determination of mineral solubilities in fluids using a hydrothermal diamond-anvil cell and SR-XRF: Solubility of AgCl in water. American Mineralogist, 88, 288–292.

Wirth, R. (2004) Focused Ion Beam (FIB): A novel technology for advanced application of micro- and nanoanalysis in geosciences and applied mineralogy. European Journal of Mineralogy, 16, 863–877.

Vekemans, B., Janssens, K., Vincze, L., Adams, F., and Van Espen, P. (1995) Comparison of several background compensation methods useful for evaluation of energy-dispersive X-ray fluorescence spectra. Spectrochimica Acta Part B: Atomic Spectroscopy, 50, 149–169.

Vekemans, B., Janssens, K., Vincze, L., Adams, F., and Van Espen, P. (2004) Analysis of X-ray spectra by iterative least squares (AXIL): new developments. X-ray spectrometry, 23, 278–285.

Manuscript received February 20, 2006
Manuscript accepted May 1, 2006
Manuscript handled by Bryan Chakoumakos